Journal of Neuroendocrinology, 2002, Vol. 14, 778–787

Sauvagine Regulates Ca^{2+} Oscillations and Electrical Membrane Activity of Melanotrope Cells of *Xenopus laevis*

L. N. Cornelisse,*† R. Deumens,* J. J. A. Coenen,* E. W. Roubos,*‡ C. C. A. M. Gielen,† D. L. Ypey,*‡ B. G. Jenks*‡ and W. J. J. M. Scheenen*‡

Department of *Cellular Animal Physiology and †Department of Biophysics, Nijmegen Institute for Neurosciences, University of Nijmegen, Nijmegen, The Netherlands.

‡Institute of Cellular Signalling, Nijmegen, The Netherlands.

Key words: sauvagine, calcium oscillations, patch-clamp, dynamic video imaging, melanotropes.

Abstract

Ca^{2+} oscillations regulate secretion of the hormone alpha-melanphore-stimulating hormone (α-MSH) by the neuroendocrine pituitary melanotrope cells of the amphibian *Xenopus laevis*. These Ca^{2+} oscillations are built up by discrete increments in the intracellular Ca^{2+} concentration, the Ca^{2+} steps, which are generated by electrical membrane bursting firing activity. It has been demonstrated that the patterns of Ca^{2+} oscillations and kinetics of the Ca^{2+} steps can be modulated by changing the degree of intracellular Ca^{2+} buffering. We hypothesized that neurotransmitters known to regulate α-MSH secretion also modulate the pattern of Ca^{2+} oscillations and related electrical membrane activity. In this study, we tested this hypothesis for the secretagogue sauvagine. Using high temporal-resolution Ca^{2+} imaging, we show that sauvagine modulated the pattern of Ca^{2+} signalling by increasing the frequency of Ca^{2+} oscillations and inducing a broadening of the oscillations through its effect on various Ca^{2+} step parameters. Second, we demonstrate that sauvagine caused a small but significant decrease in K^+ currents measured in the whole-cell voltage-clamp, whereas Ca^{2+} currents remained unchanged. Third, in the cell-attached patch-clamp mode, a stimulatory effect of sauvagine on action current firing was observed. Moreover, sauvagine changed the shape of individual action currents. These results support the hypothesis that the secretagogue sauvagine stimulates the frequency of Ca^{2+} oscillations in *Xenopus* melanotropes by altering Ca^{2+} step parameters, an action that likely is evoked by an inhibition of K^+ currents.

In the process of cell signalling, second messengers play an important role in transducing signals from first messenger molecules, such as growth factors, neurotransmitters and hormones, into cell physiological responses like protein synthesis, secretion and contraction. For secretory cells, modulation by first messengers of the intracellular Ca^{2+} concentration ($[Ca^{2+}]_i$) is important for determining the amount of secretion. The melanotrope cell in the pituitary intermediate lobe of the amphibian *Xenopus laevis* is a suitable model to study regulation of the second messenger $[Ca^{2+}]_i$. When placed *in vitro*, these endocrine cells display spontaneous $[Ca^{2+}]_i$ oscillations, which are built up by repetitive increments, the Ca^{2+} steps, during the rise phase and the plateau phase of an oscillation. The plateau is followed by an exponential decline to baseline $[Ca^{2+}]_i$ (1–3). Simultaneous Ca^{2+} imaging and recording of the electrical activity showed that the Ca^{2+} oscillations are coupled to action potential bursting (3).

The Ca^{2+} oscillations in *Xenopus* melanotropes are thought to drive the secretory activity of the cell (4, 5). The melanotrope cell plays a key role in the process of adaptation of skin colour to background light intensity of the toads, because they release alpha-melanophore-stimulating hormone (α-MSH) (6–9). α-MSH secretion is a strongly regulated process, which involves the action of several neural messengers, including stimulation by sauvagine, thyrotropin-releasing hormone, acetylcholine, noradrenaline, serotonin and brain-derived-neurotrophic factor and inhibition by

Correspondence to: Wim J. J. M. Scheenen, Department of Cellular Animal Physiology, Nijmegen Institute for Neurosciences, University of Nijmegen, Toernooiveld 1, 6525 ED Nijmegen, The Netherlands (e-mail: scheenen@sci.kun.nl).

dopamine, neuropeptide Y and γ-aminobutyric acid. Secreto-stimulators have been found to increase the frequency of oscillations whereas secreto-inhibitors eliminate the oscillations (4, 5, 10, 11).

We have recently shown experimentally that buffering the $[Ca^{2+}]_i$ changes the shape, frequency and amplitude of Ca^{2+} oscillations in *Xenopus* melanotropes and that the changes in the pattern of Ca^{2+} signalling are reflected by changes in the secretory activity of these cells (12). Until now, it was unclear whether α-MSH regulatory messengers modulate the pattern of Ca^{2+} oscillations and whether such a modulation would be reflected in the electrical membrane activity. Thus, the purpose of the present study was to test our hypothesis that regulators of α-MSH secretion modulate the pattern of Ca^{2+} oscillations and electrical membrane activity. To test this hypothesis, we examined the action of the melanotrope secretagogue sauvagine, which is a homologue of mammalian corticotropin-releasing hormone (CRH). In many cell types, CRH activates the adenylyl cyclase/cyclic-AMP pathway through either the CRH receptor I or II, thereby activating protein kinase A (PKA), although in some cell types involvement of protein kinase C and InsP3 has been suggested (13–17). In *Xenopus* melanotropes, sauvagine works exclusively through the adenylyl cyclase-cAMP pathway, although the receptor subtype through which it works is presently unknown. Upon receptor activation, the frequency of Ca^{2+} oscillations increases and hormone secretion and proopiomelanocortin biosynthesis is stimulated (18–23). In the present study, it is shown that sauvagine not only increases the frequency of Ca^{2+} oscillations, but also modulates their shape and affects the properties of the action currents. Sauvagine likely acts by inhibition of K^+ channels.

Materials and methods

Melanotrope cell cultures

Young-adult *Xenopus laevis*, bred in our department according to standard procedures, were adapted to a black background under continuous illumination, at 22 °C for 3 weeks prior to the experiments. They were fed weekly with beef heart. All experiments were carried out under the guidelines of the Dutch law concerning animal welfare. Animals were anaesthetized in water containing 1% MS222 and 1.5 g/l $NaHCO_3$. To remove blood cells, animals were perfused with *Xenopus* Ringer's solution (112 mM NaCl, 2 mM KCl, 2 mM $CaCl_2$, 15 mM HEPES, 0.001% ascorbic acid, 10 mM D-glucose, pH 7.4 adjusted with NaOH) containing 1% MS222. After decapitation, neurointermediate lobes of the pituitary gland were dissected and rinsed four times in XL L15 culture medium consisting of 76% L15 medium (Life Technologies Inc., Rockville, MD, USA), 1% kanamycin solution (Life Technologies), 1% antibiotic/antimyotic solution (Life Technologies), 2 mM $CaCl_2$, and 10 mM glucose (pH 7.4). After an incubation period of 45 min in Ringer's solution without $CaCl_2$ but containing 0.25% trypsin (Life Technologies), lobes were dissociated by gentle trituration with a siliconized Pasteur's pipette. The resulting cell suspension was filtered and centrifuged for 10 min at 500 r.p.m. The pellet was resuspended in XL L15 culture medium (100 µl/lobe equivalent) and cells were plated at a round glass coverslip for Ca^{2+} imaging studies, or at the centre of a plastic Petridish (Nunc, Roskilde, Denmark) for patch-clamp experiments, both coated with poly L-lysine ($M_w > 300$ kDa, Sigma, Steinheim, Germany) at a density of approximately 10 000 cells/dish. After the cells had been allowed to attach for 1 h, 2 ml XL L15 culture medium containing 10% fetal bovine serum was added to each dish. The cells were cultured for 3 days at 22 °C in a humidified atmosphere before experimental use.

Intracellular calcium measurements

Coverslips were placed in a Leiden chamber (24) and cells were loaded with either indo-1/AM (5 µM) or fura-2/AM (2 µM) for 25 min after exchanging the XL L15 culture medium with a loading solution that consisted of *Xenopus* Ringer's solution (112 mM NaCl, 2 mM KCl, 2 mM $CaCl_2$, 15 mM HEPES, 10 mM glucose, 3% bovine serum albumin, pH 7.4 adjusted with NaOH) containing the fluorescent dye and 0.025% Pluronic F127. Subsequently, cells were washed twice with Ringer's solution and incubated for 15 min.

Indo-1 experiments

The Leiden chamber was placed on a NIKON diaphot inverted microscope (Nikon, Tokyo, Japan), using a NIKON ×40 water-immersion, 1.2 NA fluor objective lens, attached to an OZ confocal laser scanning microscope (Noran Instruments, Middleton, WI, USA). Excitation of indo-1 (at 351 nm) was provided by a high power Argon-ion laser (Coherent Enterprise, Santa Clara, CA, USA) and indo-1 fluorescence emission was monitored at 405 nm and 485 nm after separation with a 455-nm DCLP dichroic mirror, using a slid-width of 100 µm (25). Images (512 × 480 pixels) were collected at 30 Hz and a pixel dwell time of 100 ns. Ratio images (F405/F485) were calculated using the Intervision 2D software package (Noran Instruments).

Fura-2 experiments

The Leiden chamber was placed on a Zeiss Axiovert 135 TV (Zeiss, Oberkochen, Germany), using a Zeiss ×40 oil-immersion, 1.3 NA fluor objective lens, attached to a Coolsnap fx monochrome digital camera (Roper Scientific, Tucson, AZ, USA). Excitation wavelengths of 340 nm and 380 nm were provided by a 150-W Xenon lamp (Ushio UXL S150 MO, Ushio, Tokyo, Japan) that was mounted in a Till Photonics Polychrome IV monochromator (spectral range 320–680 nm, band width 8–15 nm; Martinsried, Germany) and led into the microscope through an optical fibre. Fura-2 fluorescence emission was monitored at 515 nm, using a 440-nm DCLP dichroic mirror in front of the camera. Image acquisition and computation of ratio images (F340/F380) was operated through Metafluor v.4.5 (Universal Imaging Corporation, Downingtown, PA, USA). Camera acquisition time was 50 ms. To obtain a maximal image acquisition speed of 1.5 Hz, a camera pixel binning of 4 × 4 pixels was performed, leading to final images of 325 × 257 pixels. Different concentrations of sauvagine (Bachem, Bubendorf, Switzerland) were applied to the cells using a peristaltic pump-controlled perifusion setup.

Patch-clamp experiments

For the recordings, an EPC-9 patch-clamp amplifier (HEKA, Lambrecht/Pfaltz, Germany) was used. Data was filtered by a Bessel filter set at 12.9 kHz. Electrical activity was monitored using a digital chart recorder (PowerLab/4sp, ADInstruments, Castle Hill, Australia). Data was stored on videotapes using a VR-10B digital data recorder (InstruTECH, New York, NY, USA) in combination with a video cassette recorder (JVC, Tokyo, Japan), which made it possible to replay the recordings and to sample individual spikes with frequencies of up to 47.2 kHz. Patch pipettes with a resistance between 4 and 8 MΩ were pulled from Wiretrol II glass capillaries (Drummond Scientific Company, Broomall PA, USA) using a Narishige PP-83 pipette puller (Narishige Scientific Instrument Laboratories, Tokyo, Japan). The cells were superfused alternately with Ringer's and a test compound (4×10^{-6} M sauvagine or 2 mM 8-Br-cAMP (Sigma) in Ringer's solution), using an 8-channel valve (Hamilton, Bonaduz, Switzerland). The superfused solution was applied by a small tube placed at a distance of 2–3 mm from the cells. In this way mechanical effects on the cells due to imposing fluid flow were prevented.

Whole-cell voltage-clamp

K^+ and Ca^{2+} currents were measured in the whole-cell voltage-clamp configuration. Voltage steps from a holding potential of −80 mV to 10 mV were applied with a duration of 250 ms (Ca^{2+}) or 400 ms (K^+) and a time interval of 10 s. Records were corrected for leak (P/N = 4). Series resistances were 14 ± 6 MΩ and membrane capacitances 9 ± 2 pF (mean ± SD). To selectively record K^+ currents, the intracellular solution consisted of 100 mM KCl, 2 mM $CaCl_2$, 1.8 mM $MgCl_2$, 0.2 mM MgATP, 10 mM EGTA, 10 mM HEPES (pH set to 7.4 with KOH) and the extracellular solution

of 112 mM Na Cl, 2 mM KCl, 2 mM $CoCl_2$, 15 mM HEPES, 10 mM glucose and 1 TTX (pH set to 7.4 with NaOH). For selective Ca^{2+} current recordings, these solutions were 100 mM CsCl, 2 mM $CaCl_2$, 10 mM EGTA, 2 mM MgATP and 10 mM HEPES (pH set to 7.3 with CsOH), and 10 mM $CaCl_2$, 15 mM HEPES, 90 mM TEACl and 2 mM $MgCl_2$ (pH set to 7.4 with TEAOH), respectively.

Whole-cell current-clamp

Spontaneous electrical activity of the membrane potential was measured in the whole-cell current-clamp patch configuration with the injected current clamped to zero. Pipettes were filled with intracellular solution (100 mM KCl, 1 mM $CaCl_2$, 2 mM $MgCl_2$, 1 mM EGTA and 10 mM HEPES (pH set to 7.4 with KOH). The bath contained *Xenopus* Ringer's solution.

Cell-attached-patch action current recording

Electrical activity was recorded in the cell-attached-patch (CAP) voltage-clamp mode at zero pipette potential, as described previously (3). This configuration has two distinct advantages for the study of spontaneous firing activity, namely an absence of transmembrane leaks and the maintenance of the cytoplasmic composition. In this configuration, the measured current (I_{CAP}) is the sum of the capacitive current ($I_C = C_{CAP}dV/dt$, where C_{CAP} is the capacitance of the patch, and V the membrane potential) through the patch and the gated current through the channels (I_{ch}) that are present in the patch (26, 27). Action potentials cause biphasic current events (action currents) in the cell-attached patch. This biphasic shape is mainly due to the capacitive current, which is shaped as the first derivative of the action potential. All cell-attached-patch recordings were made with a seal resistance of 80 MΩ and at a pipette potential of 0 mV. Bath and pipettes were filled with *Xenopus* Ringer's solution.

Data analysis

Intracellular calcium measurements

Analysis of the ratio values of the Ca^{2+} imaging experiments was performed off-line using Origin 6.1 (Microcal, Northampton, MA, USA). Oscillation frequency and Ca^{2+} step parameters were analysed according to Scheenen *et al.* (1) and Koopman *et al.* (2, 12, 25), respectively. All data were tested for significance with a paired Student's t-test, with $\alpha = 5\%$, using Statistica 99 (StatSoft Inc., Tulsa, OK, USA).

Whole-cell voltage-clamp

Whole-cell voltage-clamp data was analysed by calculating two variables from the current response upon a voltage step: the peak current (maximal amplitude of the evoked current between 1% and 12% of the pulse time) and the sustained current (average of values of the evoked current between 94% and 99% of the pulse time). These variables were corrected for drift due to rundown of the currents. A linear function ($y = a \times t + b$) was fitted through the control segments before and after the sauvagine segment, and the variables were multiplied with the inverse of this function times the y-axis intersect [$b/(b + a \times t)$]. For each superfusion segment, an average value for peak and for sustained current was calculated, taking into account a wash-in and wash-out time of 100 s for sauvagine.

Cell-attached-patch action current recording

Action current (spike) frequency under different situations (Ringer's, sauvagine, 8-Br-cAMP) was determined taking into account a wash-in time of 45 s and a wash-out time of 90 s. The results were normalized with respect to the control segment under Ringer's. Data of cells that showed a clear response of the electrical activity to sauvagine were analysed at a sampling time resolution of 20 kHz. Action currents were selected and the background current per spike was determined by averaging the signal between 100 and 50 ms before the positive peak of the spike. Four parameters were calculated to characterize the shape of the action current: (i) amplitude of the positive peak (positive peak minus background current); (ii) bump value (average of the current between 35% and 65% of the time interval between positive and negative peak, minus background current); (iii) amplitude of negative peak (negative peak minus background current); and (iv) action current width (time between positive and negative peak).

Statistical analysis

To test for statistical significant effects, a (paired) Student's t-test was used. For all electrophysiological experiments, analysis software was developed in Matlab 5.3 (Math Works Inc., Natick, MA, USA).

Results

Intracellular calcium imaging

We determined the responses in intracellular Ca^{2+} oscillations of melanotrope cells upon adding various concentrations of sauvagine. We have reported that the oscillation frequency remains constant during periods up to 30 min (10). Moreover, it was demonstrated that sauvagine increases the oscillation frequency (28). Our current experiments, which have a higher temporal resolution up to video speed, reveal heterogeneity in responses, both for the concentration of sauvagine at which the cells responded, and for the type of response observed (Fig. 1). At the lowest concentration of 10^{-9} M, approximately one-half of the cells (five out of 11) responded (Table 1). Of these cells, four showed an increase in oscillation frequency (e.g. Fig. 1A), whereas one cell showed a slight broadening of the Ca^{2+} oscillations (not shown). At an intermediate sauvagine concentration (10^{-8} M), 75% of the cells (18 out of 24) responded to sauvagine: in 16.7% of the cells that were initially nonoscillating, oscillations were induced (Fig. 1B); in 12.5% of the cells, the frequency of the oscillations increased (Fig. 1C); whereas in 45.8% of the cells, broader oscillations were induced (Fig. 1D). At a sauvagine concentration of 4×10^{-8} M, 92.5% of the cells responded (11 out of 12), the vast majority with a broadening of the oscillations (Fig. 1E), whereas in one cell, a frequency increase was observed (not shown). A similar broadening of the Ca^{2+} oscillations was observed when the highest tested concentration sauvagine of 4×10^{-6} M was added (Fig. 1F) ($n = 5$).

We subsequently quantified the following parameters of the Ca^{2+} steps that underlie the Ca^{2+} oscillations (25): step amplitude (sa), step interval (Δt), number of steps per oscillation (steps/osc) and the decline time constant (τ) at the end of an oscillation, fitted by a mono-exponential curve (Fig. 2B). Previous studies (3, 25) showed that, under control conditions, the variability of these parameters within a single cell is small, implying a relatively stable spontaneous oscillation behaviour.

The cell shown in Fig. 2(A) responded to 10^{-8} M sauvagine with a broadening of the oscillations. In this cell, we observed a 17% decline in sa upon sauvagine application ($P < 0.05$), a 136% increase in steps/osc ($P < 0.05$) and a 15% increase in τ ($P < 0.05$). Analysing these parameters for all cells that responded with a broadening of the oscillations following 10^{-8} M sauvagine application ($n = 13$, Fig. 2C) demonstrated a large intercellular variability for τ: an increase was observed in three cells, τ decreased in five cells and no change was observed in 5 cells. The parameters sa and steps/osc showed significant changes in all cells: sa was reduced following sauvagine treatment by $11.2 \pm 1.2\%$ ($P < 0.05$) whereas steps/osc was increased by $65.7 \pm 9.2\%$ ($P < 0.01$). Therefore, the broadening of the oscillations is caused by an

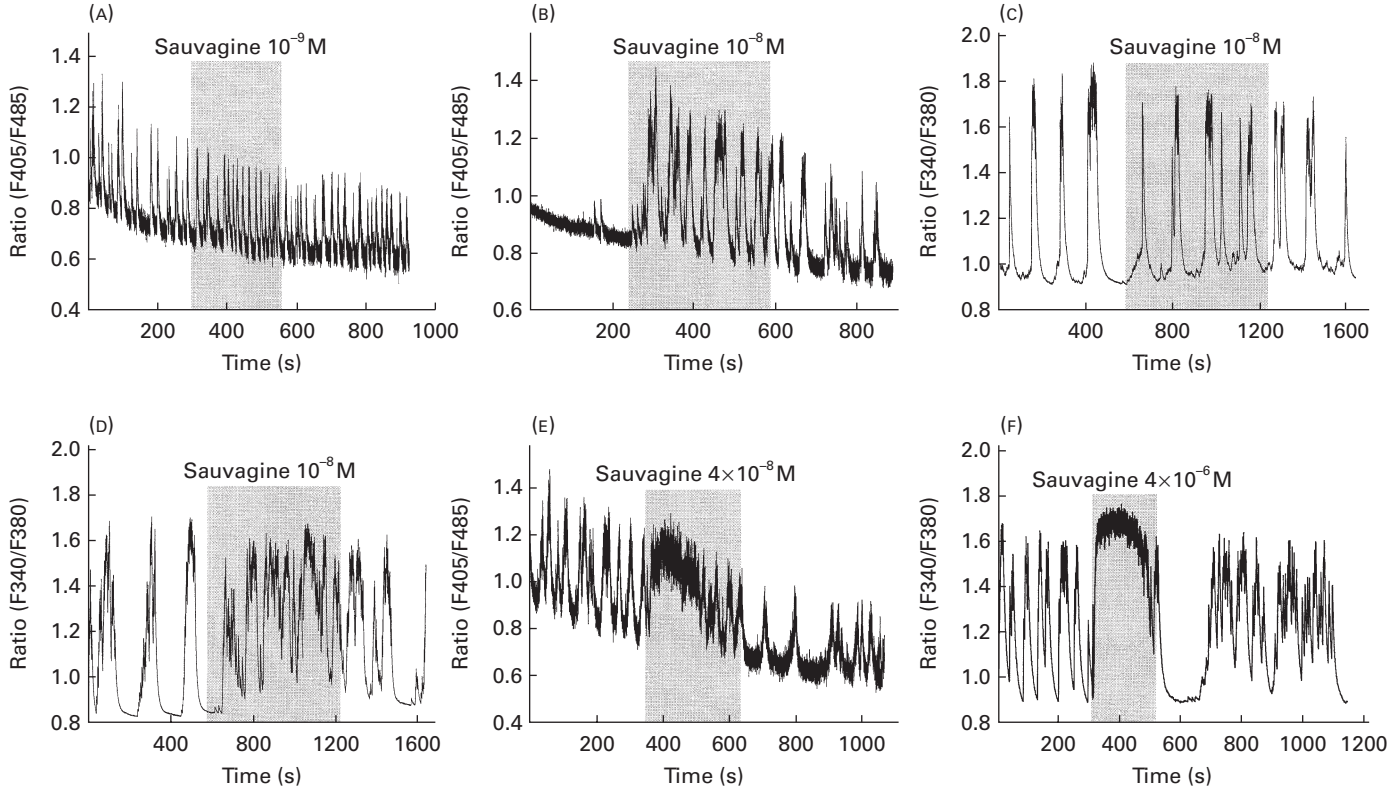

FIG. 1. Different responses of Ca^{2+} oscillations to sauvagine. (A) Increase in frequency at 10^{-9} M. (B) Induced oscillations at 10^{-8} M. (C) Increase in frequency at 10^{-8} M. (D) Broadening of oscillations at 10^{-8} M. (E) Broadening of oscillations at 4×10^{-8} M. (F) Broadening of oscillations at 4×10^{-6} M.

TABLE 1. Classifications of Responses in Ca^{2+} Oscillations of *Xenopus* Melanotropes to Sauvagine at Different Concentrations.

	Response (%)				
Concentration	n	Broader	Increased frequency	Induced	No effect
1×10^{-9} M	11	9	36.4	–	54.6
1×10^{-8} M	24	45.8	12.5	16.7	25.0
4×10^{-8} M	12	85.0	7.5	–	7.5

n, total number of cells observed at each concentration. See Results for a description of responses.

increase in the number of steps per oscillation and not by an increase in the time between steps.

Patch-clamp experiments

Spontaneous Ca^{2+} oscillations in *Xenopus* melanotropes are driven by electrical activity of the plasma membrane (3). To investigate whether and how sauvagine acts on the Ca^{2+} oscillations by affecting this activity, different types of patch-clamp experiments were performed.

Effect of sauvagine on Ca^{2+} and K^+ currents in whole-cell voltage-clamp

The stimulatory action of sauvagine on the intracellular calcium oscillations could be due to a stimulatory effect of this secretagogue on action potential firing (e.g. by potentiating Ca^{2+} currents, and/or by depressing K^+ currents). Therefore, whole-cell voltage-clamp studies were performed to test the effect of sauvagine on these currents. The results of these experiments for both Ca^{2+} and K^+ currents are shown in Fig. 3(A,B). The left panels are examples of recordings of peak (1, open circle) and sustained (2, closed circle) currents, corrected for leak and rundown. The insets indicate the current responses to voltage steps from -80 mV to $+10$ mV (with durations of 250 ms and 400 ms for Ca^{2+} and K^+, respectively) and the definition of peak and sustained currents. Sauvagine (4×10^{-6} M) has no effect on Ca^{2+} peak (1) and sustained (2) current (Fig. 3A, right panels). The average control peak current of all cells (n = 9) was -363 ± 50 pA (SEM), -366 ± 44 pA (SEM) in the presence of sauvagine and -353 ± 50 pA (SEM) after wash-out of sauvagine. For the sustained current, these values were -264 ± 38 pA (SEM), -261 ± 35 pA (SEM) and -247 ± 37 pA (SEM), respectively.

In the right panels of Fig. 3(B), a small but significant inhibiting effect of sauvagine on both K^+ peak (1) and sustained (2) currents is shown. The average peak current of

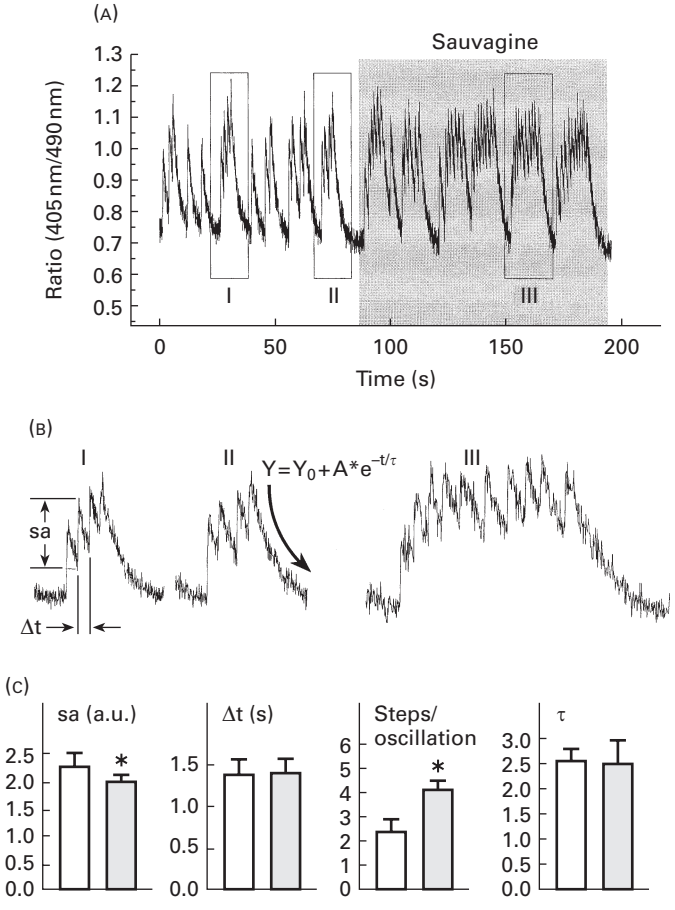

FIG. 2. Effect of 10^{-8} M sauvagine on oscillation parameters in an example of a melanotrope cell that responded with a broadening of the Ca^{2+} oscillations. (A) Total record. (B) Enlargements of Ca^{2+} peaks in record sections indicated by Roman capitals in (A). Oscillation parameters in the records: step amplitude (sa), time between steps (Δt), and decline time constant (τ). (C) Statistical results of the Ca^{2+} oscillation parameters of all cells (*$P<0.05$).

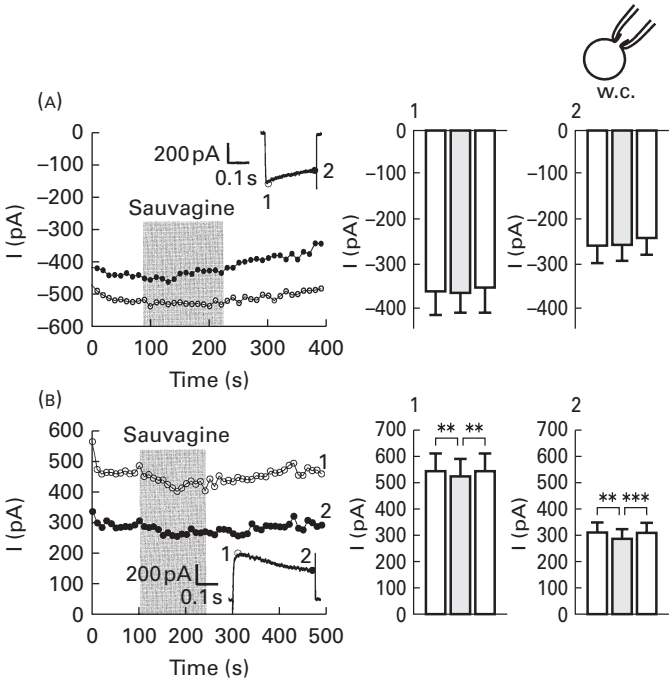

FIG. 3. Effect of 4×10^{-6} M sauvagine on (A) Ca^{2+} currents, and (B) K^+ currents, measured in whole-cell voltage-clamp. Insets show typical current responses to a voltage step from -80 to 10 mV (with durations of 250 ms and 400 ms for Ca^{2+} and K^+, respectively) and the definition of peak (1) and sustained (2) currents. Left panels show typical recordings of peak and sustained currents. Right panels show statistical results for (1) peak and (2) sustained currents (n = 9 for Ca^{2+} currents, n = 8 for K^+ currents) (**$P<0.01$, ***$P<0.001$).

all cells (n = 8) decreased from 542 ± 67 pA to 521 ± 67 pA ($P<0.01$) after superfusion of sauvagine and recovered again to 544 ± 67 pA ($P<0.01$) after washout of sauvagine. The sustained current values were 315 ± 39 pA, 292 ± 35 pA ($P<0.01$), and 314 ± 37 pA ($P<0.001$), respectively.

The general conclusion of these melanotrope whole-cell current experiments is that neither the activation nor inactivation process of the Ca^{2+}channels is affected, whereas both processes are slightly affected with respect to the K^+ channels.

Effect of sauvagine on action potential firing in whole-cell current-clamp

Considering the small effect of sauvagine on K^+ currents and the absence of an effect on Ca^{2+} currents, it could be that the whole-cell configuration disturbs the intracellular signalling pathways of sauvagine. To test for such a whole-cell induced artifact, whole-cell current-clamp experiments monitoring action potentials were performed (n = 11). We observed various patterns of electrical activity that differed both within a cell and among cells. The most commonly observed patterns consist of high-frequency tonic firing (Fig. 4A) or of bursts of high-frequency action potentials (Fig. 4B).

In four out of 11 cells sauvagine (4×10^{-6} M) did not induce a change in electrical activity (Fig. 4A). In six cells, an increase in activity in the form of burst spiking was observed (Fig. 4B), while one cell showed an increased firing frequency. In five cells, the activity was reduced after washout of sauvagine (Fig. 4B) but none of these cells returned to the firing pattern as observed before sauvagine treatment. In four cells, spontaneous electrical activity disappeared after wash-out of sauvagine.

Enlargements of segments of the different patterns are presented in Fig. 4(C). The following patterns were distinguished: (i) continuous firing of action potentials (1–2 Hz) with strong afterhyperpolarization to -60 mV (continuous spiking, n = 3); (ii) firing of single action potentials (0.5–2 Hz) on top of a slow oscillating wave (single spiking, n = 6); (iii) firing of multiple high-frequency action potentials (4–10 Hz) from a plateau (burst spiking, n = 8); and (iv) slow oscillations (subthreshold oscillations, n = 4). In one of the 11 cells, broad depolarizations ('plateau potentials', (v), not shown) were observed during sauvagine treatment. Patterns (i), (ii) and (iii) were seen under both control and sauvagine conditions. Pattern (iv) was only observed under control conditions. Patterns (iii) to (v) do not correspond to any of the typical Ca^{2+} step patterns that occur in oscillating *Xenopus*

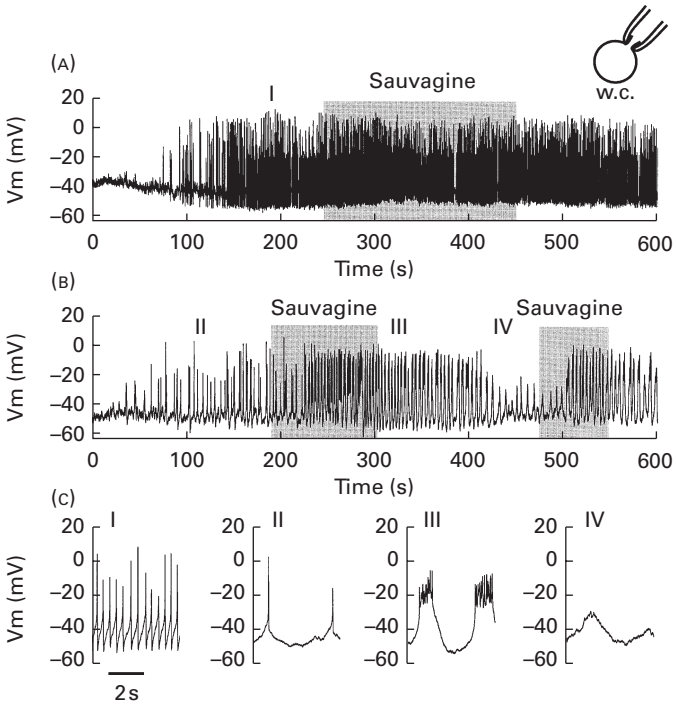

FIG. 4. Effect of sauvagine (4×10^{-6} M) on the electrical activity measured in whole-cell current-clamp. (A) Example of a nonresponding cell. (B) Example of a responding cell. (C) Stretched-out record segments illustrating various types of electrical activity observed in (A) and (B): (I) continuous spiking, (II) single spiking, (III) burst spiking and (IV) subthreshold oscillations.

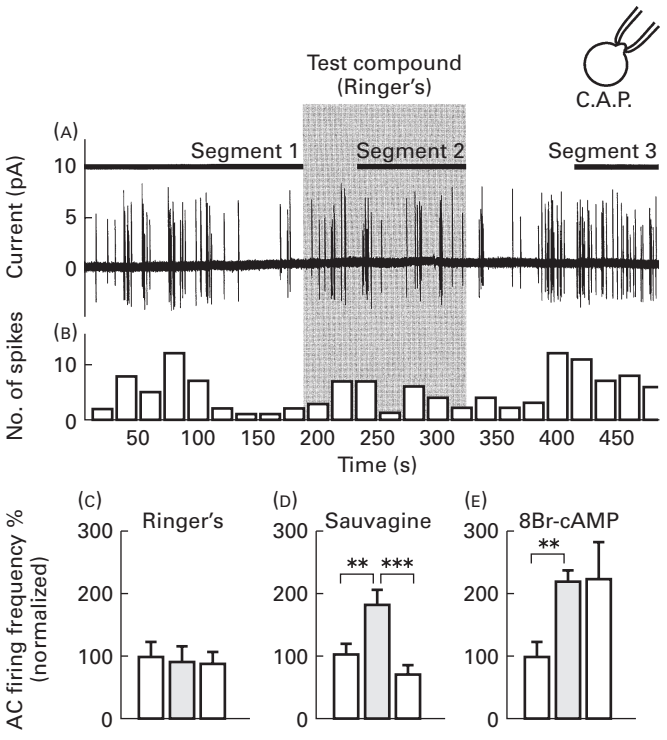

FIG. 5. Effect of test solutions on the action current firing in cell-attached-patch voltage-clamp. (A) Action currents. Horizontal bars indicate the superfusion segments minus the wash-in and wash-out times of the test solution (Ringer's in this case) to determine the action current spike frequency. (B) Spikes binned in 20-s time intervals. (C) Effect of Ringer's on average action current spike frequency (n = 8). (D) Effect of sauvagine on average action current spike frequency (n = 21). (E) Effect of 8-Br-cAMP on average action current spike frequency (n = 5) (action current spike frequencies in (C) to (E) are normalized with respect to the control segments (**P < 0.01, ***P < 0.001).

melanotropes (3). We did not observe bursts consisting of 3–10 spikes with an interspike interval of approximately 1 s (clustered spiking), which were expected based on the general Ca^{2+} oscillation patterns and cell-attached patch recordings performed previously (3).

In conclusion, no consistent effect of sauvagine could be determined on the membrane-potential activity, measured in the whole-cell current-clamp configuration. Moreover, in this configuration, various patterns of electrical activity were observed that did not correspond to the general Ca^{2+} step patterns of oscillating *Xenopus* melanotropes cells.

Effect of sauvagine and 8-Br-cAMP on action current firing in the cell-attached-patch mode

The absence of consistent effects of sauvagine on action potential firing might be due to the fact that the used whole-cell configuration causes wash-out of intracellular components which may be necessary to maintain action potential bursting. To avoid such possible artifacts, the less invasive cell-attached-patch technique was used to measure the effect of sauvagine on spontaneous firing of the melanotrope cell as seen as action currents in the patch. In this configuration, the cell membrane remains intact, which prevents disturbance of the cytoplasm.

To determine the variability in the spontaneous firing of the melanotrope cells in the cell-attached-patch mode and to establish the reliability of the superfusion procedure, we performed control experiments (n = 8) with *Xenopus* Ringer's solution. A representative example is presented in Fig. 5(A). The horizontal bars indicate the superfusion segments minus the initial wash-in and wash-out times, used to determine the number of spikes per 100 s. Figure 5(B) shows the spikes of Fig. 5(A) binned in time intervals of 20 s. A large variability in firing patterns among cells was observed. The patterns varied from bursting firing with a low frequency at 20–40 spikes per 100 s (n = 2), to continuous high-frequency spiking at 80–180 spikes per 100 s (n = 2). Some cells switched between these patterns (n = 4). All patterns could be related to types of Ca^{2+} step patterns generally seen in melanotrope cells (3) where low-frequency bursting firing corresponds to oscillations of a few steps and continuous spiking corresponds to long plateaus consisting of many steps. Despite this large variability, the results in Fig. 5(C) show that the superfusion procedure does not affect the spontaneous firing of the cells. The mean action current spike frequency normalized to the first segment for all cells measured (n = 8) was $100 \pm 22\%$ for segment 1, $90 \pm 24\%$ for segment 2 and $88 \pm 19\%$ for segment 3.

The effect of 4×10^{-6} M sauvagine on the electrical activity in the cell-attached-patch under voltage-clamp at zero pipette potential was tested in 21 cells. Figure 6(A) is a typical

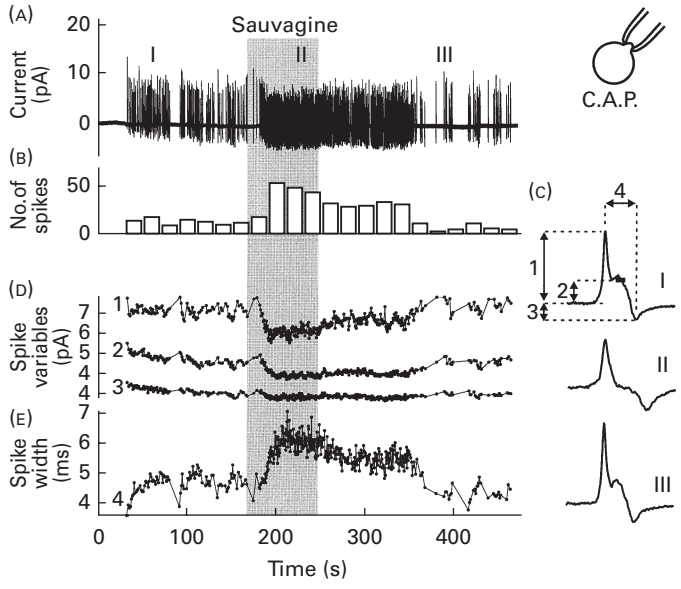

FIG. 6. (A) Action currents measured in the cell-attached-patch configuration. (B) Spikes binned in 20-s time intervals. (C) Action currents sampled with 0.05 ms time resolution. Roman capitals correspond to location of the spikes in the trace in (A). Arabic numbers denote the spike parameters: (1) positive peak; (2) bump value; (3) negative peak; and (4) spike width. (D) Spike parameters 1–3 as a function of time; note that spike amplitudes in (A) are smaller than those in (D) due to the low sampling resolution used in (A). (E) Spike width as a function of time.

recording of action currents measured during such experiments. The vertical grey bar indicates application of sauvagine. In the first superfusion segment, the cell spontaneously fires action currents. Upon adding sauvagine in the second segment, an increase in the firing frequency is observed after 20 s. After switching back to *Xenopus* Ringer's solution in the third segment, the cell returns to low frequency firing in a bursting manner after 100 s. In Fig. 6(B), the spikes of the recording shown in Fig. 6(A) are binned in 20 s intervals. The effect of sauvagine is clearly visible as a three-fold increase in the number of spikes per bin.

The results for all 21 cells are shown in Fig. 5(D). As in the control experiments, different cells showed a large variability in firing pattern and frequency. Nevertheless, sauvagine clearly increases the mean spontaneous action current firing normalized to segment 1 from $100 \pm 15\%$ to $178 \pm 25\%$ ($P < 0.01$). The effect is reversible as spiking decreases to 68 ± 14 ($P < 0.001$) after wash-out of sauvagine.

In previous studies, it was demonstrated that sauvagine increases the frequency of Ca^{2+} oscillations through a cAMP/PKA-dependent mechanism (22). Therefore, we tested the effect of 2 mM 8-Br-cAMP on electrical activity ($n = 5$). After switching to 8-Br-cAMP, the action current firing sharply increased from $100 \pm 22\%$ to $219 \pm 20\%$ (Fig. 5E) ($P < 0.01$). This effect was not reversible because switching back to Ringer's yielded a mean of $225 \pm 57\%$.

In conclusion, both sauvagine and 8-Br-cAMP increase action current firing as measured in the cell-attached patch mode. This effect only is reversible for sauvagine.

Effect of sauvagine on the action current shape

Changes in action potential firing, caused by changes in the electrical properties of the membrane (e.g. changes in channel activation) imply changes in the shape of the action current (I_{CAP}) recorded in the cell-attached patch mode. First, the gated current through the channels in the patch (I_{ch}) can be changed and, second, the capacitive current of the patch (I_C) can be changed due to a different shape of the underlying action potential. To see whether the action current shapes were affected by sauvagine, two cells were studied in which the action current frequency showed a strong increase upon sauvagine addition. Figure 6(C) shows three examples of spikes sampled with a 0.05-ms time resolution from the three segments in the trace in Fig. 6(A). The action current taken from the sauvagine segment differs from the action currents taken from the control segments. It does not reveal the bump that is present in the control spikes between the positive peak and negative peak and it is wider. Four parameters that characterize the action current shape are indicated in spike I of Fig. 6(C): (i) amplitude of the positive peak; (ii) bump value; (iii) amplitude of negative peak; and (iv) action current width. In Fig. 6(D,E), these parameters are shown as a function of time. A clear effect is visible on the positive peak, negative peak, bump value and action current width. Statistical results for both cells were similar and are shown in Table 2. The positive peak was reduced by sauvagine by 15–30% and recovered under Ringer's to 99–108% of the original amplitude under control conditions. The negative peak was increased by 24–30% to more negative values under sauvagine and remained at 121–126% under subsequent Ringer's application. The bump value decreased by 90–98% under sauvagine and recovered under Ringer's solution to 49–60% of the bump value under control conditions. Finally, the spike width increased with 30–40% under sauvagine and recovered under Ringer's to 104–120% of the original width. All these changes are statistically significant.

Thus, there is a sauvagine-induced increase in melanotrope spike frequency associated with changes in the shape of the action currents, measured via the cell-attached-patch technique.

Discussion

Effect of sauvagine on calcium oscillation patterns and step kinetics

In this study, we tested the hypothesis that neural messengers modulate Ca^{2+} oscillation patterns and Ca^{2+} step kinetics in *Xenopus* melanotrope cells. It was previously shown that the secretagogue sauvagine increases the frequency of Ca^{2+} oscillations in *Xenopus* melanotrope cells (4, 28). Using high temporal resolution confocal laser scanning microscopy and digital imaging microscopy, we now show that sauvagine is capable of inducing an additional response, namely broadening the oscillations by inducing more Ca^{2+} steps per oscillation. This response is cell- and dose-dependent, with low concentrations of sauvagine predominantly increasing the frequency of the oscillations and high concentrations leading to a broadening of the oscillations. At a moderate sauvagine

concentration (10^{-8} M), both responses were observed. When the sauvagine concentration was maximal (4×10^{-6} M), only a broadening of the Ca^{2+} response was seen with an increase in the number of steps, without affecting the time interval between steps. The ability of sauvagine to induce different intracellular responses may allow this neuropeptide to orchestrate different cellular responses. For example, it is known that sauvagine not only stimulates the secretion of α-MSH from the *Xenopus* melanotrope cell (18), but also induces the expression of the precursor protein pro-opiomelanocortin (23). We speculate that an increase in oscillation frequency only leads to an increase in secretion, whereas broadening of oscillations stimulates both pro-opiomelanocortin (POMC) gene expression and α-MSH secretion.

Previous studies have shown that several Ca^{2+} steps build up Ca^{2+} oscillations in *Xenopus* melanotropes (1–3). In theory, the shape of Ca^{2+} oscillations could be changed by changing the amplitude of each step, the time interval between steps and the number of steps in each oscillation, or by changing the speed with which Ca^{2+} is extruded from the cell as $[Ca^{2+}]_i$ returns to its basal value. Based on our results, we conclude that sauvagine can change the shape of an oscillation by influencing the number of steps in an oscillation. We have recently demonstrated that increasing the Ca^{2+} buffering capacity in the *Xenopus* melanotrope leads to broader oscillations as a consequence of the oscillations having more steps, more time between steps and slower Ca^{2+} extrusion kinetics (12). The fact that sauvagine does not reduce the Ca^{2+} extrusion kinetics in a consistent way argues against an effect of this secretagogue on Ca^{2+} buffering mechanisms. A possible target of sauvagine would be the electrical membrane activity, because we have previously shown that the steps are likely driven by the action of a plasma membrane potential oscillator (22) that probably consists of Ca^{2+}, Na^+, K^+ and 'leak' channels (29). Therefore, the effect of sauvagine on whole-cell Ca^{2+} and K^+ currents and action potential firing was investigated using whole-cell and cell-attached patch-clamp configurations, respectively.

Effect of sauvagine on Ca^{2+} and K^+ currents in the whole-cell voltage-clamp mode

The stimulatory action of sauvagine on the Ca^{2+} oscillations may be due to stimulation of Ca^{2+} currents, inhibition of K^+ currents and/or stimulation of Na^+ channels. In our experiments on Ca^{2+} and K^+ currents, only a small, but consistent inhibition on K^+ currents was observed. These results suggest that either sauvagine does not act primarily via Ca^{2+} or K^+ currents, but that it acts on other membrane ion channels, such as Na^+ currents, or that it affects the electrical currents through a soluble factor, which could be lost in the whole-cell configuration. cAMP is a likely candidate for a soluble factor, because it was demonstrated that sauvagine stimulates the *Xenopus* melanotropes by activating adenylyl cyclase (18–22). This is in agreement with the observation that CRH regulates the Ca^{2+} signalling in corticotropes via the adenylyl cyclase/cAMP pathway, subsequently affecting K^+ and Ca^{2+} currents (30–34). The

TABLE 2. Values for Spike Parameters (with SEM) Under Ringer's (R) and Sauvagine (S).

	Positive peak (pA)			Negative peak (pA)			Bump value (pA)			Spike width (ms)		
Cell	R	S	R	R	S	R	R	S	R	R	S	R
A	1.61 (0.01)	1.13 (0.01)	1.59 (0.03)	−0.40 (0.01)	−0.52 (0.01)*	−0.51 (0.01)	0.40 (0.01)	0.01 (0.01)	0.20 (0.02)	4.70 (0.1)	6.10 (0.1)	4.90 (0.1)
B	1.26 (0.01)	1.07 (0.01)	1.36 (0.03)	−0.61 (0.02)	−0.77 (0.01)**	−0.75 (0.01)	0.66 (0.03)	0.07 (0.01)	0.40 (0.02)	5.50 (0.1)	7.80 (0.1)	6.60 (0.1)

For a definition of parameters, see Fig. 6(C). All changes with respect to the previous segment are significant with $P < 0.001$ unless indicated otherwise (*$P < 0.05$, **$P < 0.01$).

fact that no effect on Ca^{2+} currents was observed in our studies indicates that the effect of CRH or CRH homologues might be cell-specific.

Effect of sauvagine on action potential firing

The idea that a soluble factor, such as cAMP, is lost during the whole-cell patch-clamp mode is strengthened by two observations in our whole-cell current-clamp experiments. First, in these experiments, a broad repertoire of spiking patterns was observed. However, comparison between the results of the Ca^{2+} imaging studies and the whole-cell current clamp experiments shows that the frequency of the action potentials during bursting observed under whole-cell patch-clamp conditions, although qualitatively similar, is one order of magnitude higher than the frequency of the Ca^{2+} steps during Ca^{2+} oscillations. This is in contrast with our previous demonstration that a one-to-one correlation between electrical membrane bursting and Ca^{2+} steps exists, the former being measured in the cell-attached patch-clamp configuration (3). Second, although in general a slight increase in electrical activity under sauvagine was observed, this effect is not reversible. The observation that this electrical activity tends to progress from spiking to plateau bursting after superfusion of sauvagine might be explained by an inhibition of a slow K^+ current that is involved in the bursting mechanism. If such a current is inhibited, bursts become longer and the frequency of the spikes in the burst increases. However, also under sauvagine-stimulated conditions, the bursting firing patterns did not correspond to the frequencies observed during Ca^{2+} imaging experiments. These observations led us to record the electrical activity of the melanotropes in a less invasive way. Since the *Xenopus* melanotropes do not display electrical membrane bursting, but only continuous spiking using the perforated patch technique (35), we performed cell-attached-patch voltage-clamp experiments (3). Such experiments demonstrated a large intercellular variability in the spontaneous electrical activity as well as in the response of the electrical activity to sauvagine. The large variability in the response to sauvagine is in agreement with the heterogeneity observed in Ca^{2+} responses to sauvagine. Our observation that cAMP stimulates the action current frequency confirms earlier studies (22) showing that sauvagine acts by stimulating adenylyl cyclase and is unable to induce Ca^{2+} oscillations when these are inhibited by the PKA inhibitor H-89. The long-lasting effect of 8-Br-cAMP may be due to its slow intracellular breakdown.

Effect of sauvagine on action current kinetics

Analysis of several characteristics of the action currents in two cells that responded strongly to sauvagine indicates that action current shapes are affected. The increase in width of the action current implies that action potentials last longer in the presence of sauvagine. Moreover, the amplitude of the positive and negative peak as well as the bump values are also affected in the two cells analysed. A decrease in the positive peak amplitude would imply a decreased rise-speed of the action potential. Preliminary experiments indicate that the bump current is an ion channel-induced current caused by opening of individual channels in the patched membrane (L.N. Cornelisse, unpublished observation). Considering the positive sign of the bump, it most likely comprises an outward K^+ current. A decrease in the amplitude of the bump current would then reflect an inhibition of K^+ current. This could explain the delayed repolarization of the action potential causing the longer lasting action potentials as reflected by the wider action currents under sauvagine. Moreover, the inhibition of the K^+ current could result in a more depolarized membrane potential leading to an increase of action potential firing by sauvagine. Several classes of K^+ currents have been implemented in the maintenance of the membrane potential. For example, in rat corticotropes, inwardly rectifying K^+ currents are shown to be affected by CRH, leading to a subsequent membrane depolarization (32).

In conclusion, we show that sauvagine, besides affecting the frequency of Ca^{2+} oscillations in *Xenopus* melanotropes, can also affect the shape of the oscillations and therefore the pattern of Ca^{2+} signalling. Moreover, we demonstrate that sauvagine acts on the electrical activity in a similar way to its effect on Ca^{2+} oscillations. The mechanism involves the cAMP pathway and presumably reduces K^+ currents, thereby diminishing the hyperpolarizing capacity of the cell upon a burst of action potentials. The physiological consequences of these phenomena to melanotrope cell functioning with respect to secretion and POMC gene expression are currently under investigation.

Acknowledgements

We like to thank Dr W. J. H. Koopman for assistance with the confocal laserscanning microscopy, Dr E. Pearson for assistance with the digital imaging experiments, Mrs H. Zang for assistance with the Ca^{2+} current measurements, and Mr P. M. J. M. Cruijsen and Mr R. J. E. Engels for assistance during cell preparations and animal care. This project was supported by grant ALW 805-25-231 from the Dutch Foundation for Scientific Research (NWO).

Accepted 7 May 2002

References

1 Scheenen WJJM, Jenks BG, van Dinter RJAM, Roubos EW. Spatial and temporal aspects of Ca^{2+} oscillations in *Xenopus laevis* melanotrope cells. *Cell Calcium* 1996; **19:** 219–227.

2 Koopman WJH, Scheenen WJJM, Roubos EW, Jenks BG. Kinetics of calcium steps underlying calcium oscillations in melanotrope cells of *Xenopus laevis*. *Cell Calcium* 1997; **22:** 167–178.

3 Lieste JR, Koopman WJH, Reynen VJ, Scheenen WJJM, Jenks BG, Roubos EW. Action currents generate stepwise intracellular Ca^{2+} patterns in a neuroendocrine cell. *J Biol Chem* 1998; **273:** 25686–25694.

4 Shibuya I, Douglas WW. Spontaneous cytosolic calcium pulsing detected in *Xenopus* melanotrophs: modulation by secreto-inhibitory and stimulants ligands. *Endocrinology* 1993; **132:** 2166–2175.

5 Scheenen WJJM, Jenks BG, de Koning HP, Vaudry H, Roubos EW. Secretion of α-MSH from *Xenopus laevis* from melanotropes depends on calcium influx through ω-conotoxin-sensitive voltage-operated calcium channels. *J Neuroend* 1994; **6:** 457–464.

6 Jenks BG, Leenders HJ, Cruijsen P, Martens GJM, Roubos EW. Adaptation physiology: the functioning of pituitary melanotrope cells during background adaptation of the amphibian *Xenopus laevis*. *Zool Sci* 1993; **10:** 1–11.

7 Kolk SM, Kramer BMR, Cornelisse LN, Tonosaki Y, Dotman CH, Koopman WJH, Ubink WR, Scheenen WJJM, Jenks BG, Roubos EW.

Multiple control and dynamic response of the amphibian melanotrope cell. *Comp Biochem Physiol Part B* 2002; **132:** 257–260.
8 Roubos EW, Kolk SM, Kramer BMR, Cornelisse LN, Janssen MC, Scheenen WJJM, Jenks BG. Neuroendocrinology – from concepts and complexity to integration. In: Goos HJTh, Rastogi RK, Vaudry H, Pierantoni R, eds. *Perspective in Comparative Endocrinology: Unity and Diversity*. Bologna: Monduzzi Editore, 2001: 465–472.
9 Kramer BMR, Kolk SM, Berghs CAFM, Tuinhof R, Ubink WR, Jenks BG, Roubos EW. Dynamics and plasticity of peptidergic control centres in the retino-brain-pituitary system of *Xenopus laevis*. In: Gonzáles A, Smeets WJAJ, eds. *Neuropeptide Histochemistry in the Amphibian Brain, Microscopy Research and Technique.* New York: Wiley-Liss, Inc., 2001: 188–199.
10 Scheenen WJJM, Jenks BG, Roubos EW, Willems PHGM. Spontaneous calcium oscillations in *Xenopus laevis* melanotrope cells are mediated by ω-conotoxin sensitive calcium channels. *Cell Calcium* 1994; **15:** 36–44.
11 Strien FJC, Roubos EW, Vaudry H, Jenks BG. Actylcholine autoexcites the release of proopiomelanocortin-derived peptides from melanotrope cells of *Xenopus laevis* via an M1 muscarine receptor. *Endocrinology* 1996; **137:** 4298–4307.
12 Koopman WJH, Roubos EW, Jenks BG. $[Ca^{2+}]_i$ shapes Ca^{2+} oscillations in an excitable cell by regulating Ca^{2+} removal and synchronizing electrical bursting. *Pflügers Arch* 2001; **443:** 250–256.
13 Dautzenberg FM, Dietric K, Palchauhuri MR, Spiess J. Identification of two corticotrophin-releasing factor receptors from *Xenopus laevis* with high ligand selectivity: unusual pharmacology of the type 1 receptor. *J Neurochem* 1997; **69:** 1640–1649.
14 Dautzenberg FM, Kilpatrick GJ, Hauger R, Moreau J-L. Molecular biology of the CRH receptors. *Mood Peptides* 2001; **22:** 753–760.
15 Malagoli D, Franchini A, Ottaviani E. Synergistic role of camp and IP(3) in corticotropin-releasing hormone-induced cell shape changes in invertebrate immunocytes. *Peptides* 2000; **21:** 175–182.
16 Chakravorty A, Mesiano S, Jaffe RB. Corticotropin-releasing hormone stimulates P450, 17alpha–hydroxylase/17,20–lyase in human fetal adrenal cells via protein kinase C. *J Clin Endocrinol Metab* 1999; **84:** 3732–3738.
17 Kapcala LP, Aguilera G. Modulation of corticotropin-releasing hormone stimulated cyclic adenosine monophosphate production by brain cells. *Brain Res* 1995; **678:** 207–212.
18 Verburg-van Kemenade BML, Jenks BG, Cruysen PMJM, Dings A, Tonon MC, Vaudry H. Regulation of MSH-release from the neurointermediate lobe of *Xenopus laevis* by CRF-like peptides. *Peptides* 1987; **8:** 1093–1100.
19 Koning HP, Jenks BG, Huchedé B, Roubos EW. Dynamics of cyclic-AMP efflux in relation to α-MSH secretion from melanotrope cells of *Xenopus laevis*. *Life Sci* 1992; **51:** 1667–1673.
20 Koning HP, Jenks BG, Roubos EW. Analysis of $GABA_B$ receptor function in the *in vitro* and *in vivo* regulation of αMSH secretion from melanotrope cells of *Xenopus laevis*. *Endocrinology* 1993; **132:** 674–681.
21 Leenders HJ, Jenks BG, Roubos EW. Inhibition of α-MSH secretion is associated with increased cyclic-AMP egress from the neurointermediate lobe of *Xenopus laevis*. *Life Sci* 1995; **57:** 2447–2453.
22 Lieste JR, Scheenen WJJM, Willems PHGM, Jenks BG, Roubos EW. Calcium oscillations in melanotrope cells of *Xenopus laevis* are differentially regulated by cAMP-dependent and cAMP-independent mechanisms. *Cell Calcium* 1996; **20:** 329–337.
23 Dotman CH, Maia A, Jenks BG, Roubos EW. Sauvagine and TRH differentially stimulate proopiomelanocortin biosynthesis in the *Xenopus laevis* intermediate pituitary. *Neuroendocrinology* 1997; **66:** 106–113.
24 Ince C, Van Dissel JT, Diesselhoff MC. A teflon culture dish for high-magnification microscopy and measurements in single cells. *Pflügers Arch* 1985; **403:** 240–244.
25 Koopman WJH, Scheenen WJJM, Errington RJ, Roubos EW, Willems PHGM, Bindels RJM, Jenks BG. Membrane-initiated Ca^{2+} signals generate diverse spatiotemporal Ca^{2+} signals in subcellular regions of an excitable cell. *Biophys J* 2001; **81:** 57–65.
26 DeFelice LJ, Goolsby WN, Mazzanti M. Potassium channels and the repolarization of cardiac cells. *Ann NY Acad Sci* 1990; **588:** 174–184.
27 Mazzanti M, DeFelice LJ. Ca channel gating during cardiac action potentials. *Biophys J* 1990; **58:** 1059–1065.
28 Scheenen WJJM, Jenks BG, Willems PHGM, Roubos EW. Action of stimulatory and inhibitory α-MSH secretagogues on spontaneous calcium oscillations in melanotrope cells of *Xenopus laevis*. *Pflügers Arch* 1994; **427:** 244–251.
29 Cornelisse LN, Scheenen WJJM, Koopman WJH, Roubos EW, Gielen CCAM. Minimal model for intracellular calcium oscillations and electrical bursting in melanotrope cells of *Xenopus laevis*. *Neural Comput* 2001; **13:** 113–137.
30 Luini A, Lewis D, Guild S, Corda D, Axelrod J. Hormone secretagogues increase cytosolic calcium by increasing cAMP in corticotropin-secreting cells. *Proc Natl Acad Sci USA* 1985; **82:** 8034–8038.
31 Kuryshev YA, Childs GV, Ritchie AK. Corticotropin-releasing hormone stimulation of Ca^{2+} entry in corticotropes is partially dependent on protein kinase A. *Endocrinology* 1995; **136:** 3925–3935.
32 Kuryshev YA, Haak L, Childs GV, Ritchie AK. Corticotropin-releasing hormone inhibits an inwardly rectifying potassium current in rat corticotropes. *J Physiol* 1997; **502:** 265–279.
33 Ritchie A, Kuryshev YA, Childs GV. Corticotropin-releasing hormone and calcium signaling in corticotropes. *Trends Endocrinol Metab* 1996; **7:** 365–369.
34 Shorten PR, Robson AB, McKinnon AE, Wall DJN. CRH-induced electrical activity and calcium signalling in pituitary corticotrophs. *J Theor Biol* 2000; **206:** 395–405.
35 Valentijn JA, Valentijn K. Two distinct Na^+ currents control cytosolic Ca^{2+} pulsing in *Xenopus laevis* pituitary melanotophs. *Cell Calcium* 1997; **21:** 241–251.